

Gas density measurements with heavy ion beams

S. Neff,^{a)} A. Tauschwitz, C. Niemann, D. Penache, and D. H. H. Hoffmann
Gesellschaft fuer Schwerionenforschung (GSI), Planckstr. 1, 64291 Darmstadt, Germany

S. S. Yu and W. M. Sharp

Lawrence Berkeley National Laboratory (LBNL), 1 Cyclotron Road, Berkeley, California 94720

(Received 23 August 2002; accepted 11 December 2002)

High current discharge channels are a promising option for the final stage of beam transport in a heavy ion fusion reactor. The creation and the properties of the channel are studied at the *Gesellschaft fuer Schwerionenforschung* accelerator facility. This article discusses a diagnostic technique to determine the neutral gas density channel created by a laser in a neutral gas. The concept is to measure the spreading of an ion beamlet due to collisional scattering with the gas, and thereby deduce the average line-integrated gas density. The results show a density reduction near the axis, which compares favorably with one-dimensional code calculations. © 2003 American Institute of Physics. [DOI: 10.1063/1.1543652]

I. INTRODUCTION

A critical point of design for a heavy ion fusion reactor is the transport of the beam inside the target chamber towards the target in the center. While the main scheme currently studied is ballistic focusing, it has the drawback of dealing with about 100 separate beamlets, which implies severe restrictions for the design of the final focusing magnets and the chamber shielding. A possible alternative is the assisted pinch transport. In this scheme, first studied in connection with light ion beam fusion,^{1,2} a high current discharge creates a plasma channel, which with its large azimuthal magnetic field and return current compensation allows one to transport far larger beam currents than ballistic focusing.^{3–5} Therefore the corresponding reactor concept only requires two ion beams.^{3–5}

The creation of the plasma channel is a multistage process. The gas on the beam axis is heated initially by a laser pulse. This leads to an expansion and rarefaction of the gas and creates a blanket of increased gas density around the axis. In a second step a small discharge (prepulse) increases the rarefaction on the axis and in addition ionizes the gas. Finally, the main discharge is triggered and the transport channel is created. The ion beam is then injected into the channel and transported towards the target.

The created gas density profile stabilizes the discharge against kink instabilities.^{6,7} The pre-ionization guides the discharge along the beam axis and prevents breakdowns to the metallic chamber walls.

The laser pulse in our experimental setup has an energy of about 4–5 J; the energies of the prepulse and the main discharge are about 40 J and 3.1 kJ, respectively. The interval between laser and prepulse is typically 20 μ s; the interval between prepulse and the main discharge is about 10 μ s. The best ion beam transport is achieved about 5 μ s after the beginning of the main discharge, when the discharge current and, therefore, the magnetic field reaches its maximum value.

The details of the experimental setup and measurements of the transport properties of the channel can be found in our previous publication.⁸ A thorough understanding of channel dynamics is necessary to be able to create reproducible channels. While the development of the electron density can be tracked with interferometric measurements, the neutral gas dynamics require another technique, since interferometry is only sensitive to large neutral gas density gradients.

II. METHOD OF MEASUREMENT

A heavy ion beam serves as a diagnostic tool to determine the gas density. Before entering the chamber, the beam passes a pepperpot mask and is thereby shaped into several beamlets, each with a known initial intensity profile. Afterwards the beam passes the chamber and is scattered by the chamber gas. The beam intensity profile therefore undergoes a density dependent spreading. After passing the chamber the beam hits a scintillator. A digital picture of the scintillator is taken and the intensity profile of the ion beam is determined with a computer program. A comparison of the profile width with a calibration curve finally yields the gas density along the path of the beam.

A. Shaping the beam

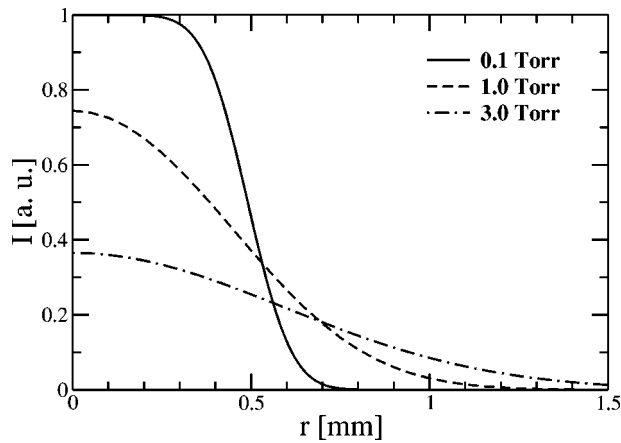
The experiments utilize the UNILAC linear accelerator facility at GSI. The heavy ion beams used have an energy of 11 MeV/u and a total current of several μ A.

When entering the chamber, the beam is shaped by a pepperpot mask. The pepperpot mask is a plate with several holes in it. Thereby the beam is split into several small beamlets. The holes have a diameter of 1 or 2 mm. The intensity of the beam varies on a larger scale; therefore the initial intensity profile of a beamlet is given by

$$I_i(r) = \begin{cases} I_{\max}, & \text{for } 0 \leq r \leq R \\ 0, & \text{for } r > R \end{cases}, \quad (1)$$

R being the radius of the hole; its center lies at $r=0$.

^{a)}Electronic mail: s.neff@gsi.de

FIG. 1. Calculated scattering profiles ($R=0.5$ mm).

B. Scattering

As the beam passes the gas in the chamber, it is scattered by the gas molecules. Since the ion beams have a high kinetic energy, small angle scattering is dominating. Starting with a point ion beam [intensity $I = \delta(r)$] results in a Gaussian profile for the scattered beam at the end of the chamber⁹

$$I(r) = I_0 \exp[-r^2/(2\sigma_r^2)], \quad (2)$$

where I_0 is the maximum intensity, r the distance from the beamlet center and σ_r the width of the profile.

The width of the profile depends on the cross section of the collision, the gas density and the distance traveled in the gas. Since the cross section for the collision cannot be easily calculated, it is derived from a reference measurement. The traveled distance corresponds to the chamber length, therefore the only remaining parameter for the beam width is the gas density. This allows the derivation of the gas density from the scatter measurement, with

$$\sigma_r \propto \sqrt{N}, \quad (3)$$

N being the gas density.⁹

Taking the initial shape of the beamlet into consideration yields a more accurate profile, which is given by the convolution of Eq. (1) with Eq. (2)

$$I_i(x, y) * I(x, y) = \int_{-\infty}^{\infty} du \int_{-\infty}^{\infty} dv I_i(x-u, y-v) \cdot I(x, y). \quad (4)$$

Numerical calculations of the integral show that for the densities used in the experiment, which are in the order of $10^{17}/\text{cm}^3$ (corresponding to a pressure of several Torr), the profiles have a Gaussian shape. The form of the hole comes into play only at very low densities (see also Fig. 1).

C. Measuring the intensity profile

After passing the chamber, the intensity profile is measured using a plastic scintillator (BC-400, 7 ns afterglow). A picture of the scintillator is taken with a high-speed digital camera. A scintillator picture with a marked beamlet is shown in Fig. 2.

The image is analyzed with a computer program (written in IDL¹⁰). Each beamlet is fitted with a two-dimensional

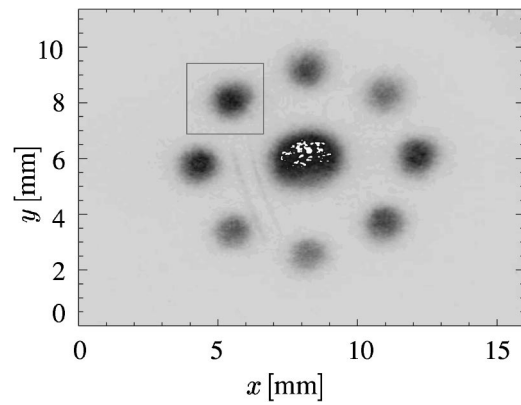


FIG. 2. Scintillator image with selected beamlet.

Gaussian distribution. This results in an averaged width for a cylindrical symmetrical gaussian distribution and a corresponding error estimate (see also Figs. 3 and 4). The gas density is then calculated from the profile width on the basis of a calibration curve.

D. Calibration curve

The calibration curve yields the relation between the gas density and the profile width. To rule out possible errors due to variations in the hole borings, a separate calibration curve is necessary for each hole of the mask. These curves are obtained by measuring the profile widths for various gas densities.

III. HYDRODYNAMICAL SIMULATION

The development of the plasma channel is simulated with CYCLOPS, a one-dimensional magnetohydrodynamical code which was written at the Lawrence Berkeley National Laboratory.¹¹ A comparison of the calculations with the measured density development allows one to test the validity of the implemented hydrodynamics. In contrast, calculations of the actual discharge depend strongly on the ionization processes which are difficult to model.

The laser absorption takes place on the nanosecond time scale while the hydrodynamic expansion proceeds in the mi-

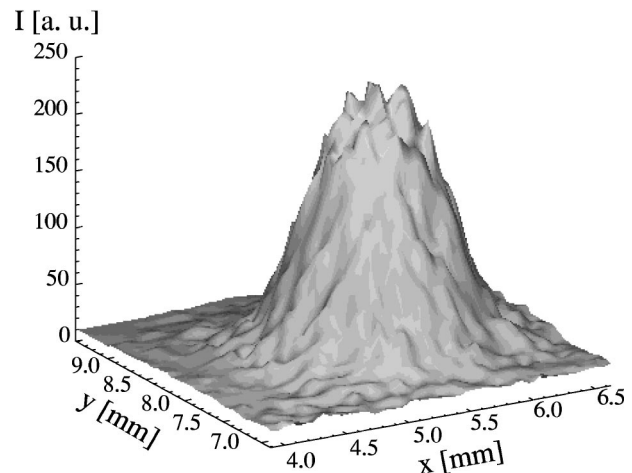


FIG. 3. Surface plot of selected beamlet.

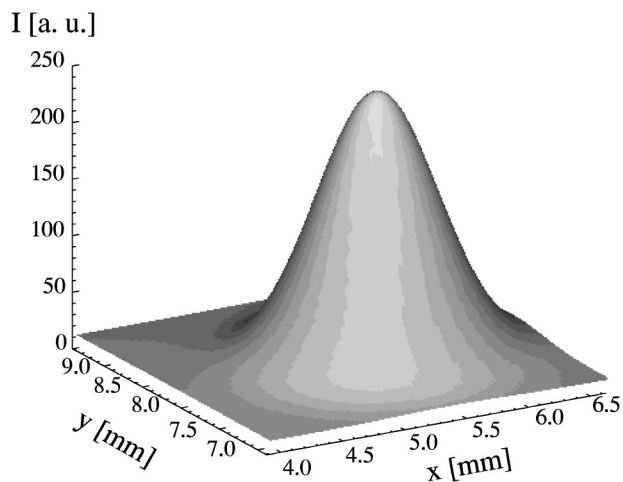


FIG. 4. Surface plot of Gaussian fit.

crosecond domain. Therefore it is justifiable to not model the complicated process of absorption itself, but instead start with a given temperature profile and homogeneous gas density.

The temperature profile has a Gaussian shape

$$T_f(r) = T_i + T_0 \cdot \exp\left[-\frac{r^2}{2\sigma_r^2}\right], \quad (5)$$

T_f being the final temperature reached after heating by the laser pulse, T_i the initial temperature of the gas (usually 300 K), r the distance from the beam axis, and σ_r the width of the profile. The profile width is set identical to the laser pulse and T_0 follows from the deposited beam energy. The pulse energy Q is equal to

$$Q = \int dV n(\mathbf{x}) \int_{T_i}^{T_f(\mathbf{x})} C_V(T) dT \quad (6)$$

$$= 2\pi L \frac{p_i}{R T_i} \int_0^\infty dr r \int_{T_i}^{T_f(r)} (C_p(T) - R) dT, \quad (7)$$

where dV is a differential volume, \mathbf{x} is the position vector for the integration, p_i is the initial pressure, and C_p the temperature dependent heat capacity of the gas (for ammonia see Ref. 12). Solving this equation numerically yields the parameter T_0 for the temperature profile. The pulse energy is determined with a calorimetric detector.

IV. COMPARISON MEASUREMENT-SIMULATION

Figure 5 shows the measurement and corresponding simulation results. The pepperpot mask used in this measurement has no hole in the center, therefore beamlets which are slightly off axis are used.

The measurements and the simulation results are in good agreement. Both indicate a steep decrease of the gas density on the axis in the first 15–20 μs . The density remains low afterwards for a long period of time and increases only slightly. Simultaneously a wall of increased gas density is created around the axis, which only slowly travels outwards.

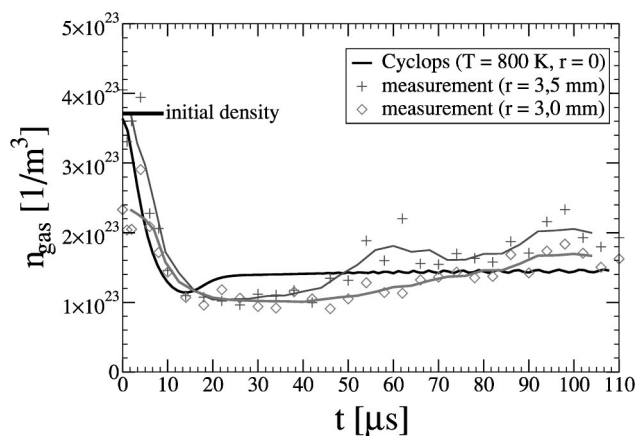


FIG. 5. Comparison of simulation and measurement for 15 mbar ammonia.

V. SUMMARY

Transport channels have a possible application as a method for final beam transport in a fusion reactor. Therefore an in-depth understanding of the channel dynamics is necessary. In order to determine the efficiency of the laser for stabilizing the discharge, a measurement of the gas density development is required. The results of measurements, which utilize the scattering of an ion beam, are compared with one-dimensional magnetohydrodynamical calculations and show a good matching.

The method has proven to be efficient for gas density measurements in the experiment. Although it cannot be applied during the discharge (the electromagnetic fields of the discharge would distort the ion beam), it is useful for getting a better understanding of the channel dynamics and verification of the simulation results. The measurements and simulation runs show that a significant rarefaction of the gas on axis can be achieved.

ACKNOWLEDGMENT

This work is supported by the German BMBF.

- ¹T. Ozaki, S. Miyamoto, K. Imasaki, S. Nakai, and C. Yamanaka, *J. Appl. Phys.* **58**, 2145 (1985).
- ²J. N. Olsen and L. Baker, *J. Appl. Phys.* **52**, 3286 (1981).
- ³A. Tauschwitz, *Fusion Eng. Des.* **493**, 32 (1996).
- ⁴S. Yu et al., in *Nuclear Instruments and Methods A* (Elsevier, Amsterdam, 1997), Vol. 415, pp. 175–181.
- ⁵A. Tauschwitz et al., in *Proceedings of the International Conference on Inertial Fusion Sciences and Applications (IFSA)*, (Elsevier, Bordeaux, France, 1999), pp. 521–526.
- ⁶W. M. Mannheimer, M. Lampe, and J. P. Boris, *Ph. Fl.* **16**, 1126 (1973).
- ⁷A. Tauschwitz, C. Niemann, D. Penache, S. Neff, R. Knobloch, R. Birkner, R. Presura, D. Ponce, and S. Yu, *Laser Part. Beams* **20** (2002).
- ⁸C. Niemann, A. Tauschwitz, D. Penache, S. Neff, R. Knobloch, R. Birkner, R. Presura, D. H. H. Hoffmann, S. S. Yu, and W. M. Sharp, *J. Appl. Phys.* **91**, 617 (2002).
- ⁹J. D. Jackson, *Classical Electrodynamics* (Wiley, New York, 1998).
- ¹⁰Written in the Interaction data Language (Research Systems, Boulder, CO 1999).
- ¹¹E. Henestroza, S. Yu, M. C. Vella, and W. M. Sharp, in Ref. 4, pp. 186–192.
- ¹²*Ullmann's Encyclopedia Of Industrial Chemistry*, edited by W. Gerhartz, (VCH, 1985), Vol. A2.